ACES Asian Chemical Editorial Society

doi.org/10.1002/asia.202300900

CHEMISTRY AN ASIAN JOURNAL Research Article

www.chemasianj.org

Effects of Size and Asymmetry on Catalase-Powered Silica Micro/nanomotors

Jun Sun,[a] Jie Wu,*[a] and Huangxian Ju[a]

Enzyme-powered micro/nanomotors that can autonomously move in biological environment are attractive in the fields of biology and biomedicine. The fabrication of enzyme-powered micro/nanomotors normally focuses on constructing Janus structures of micro/nanomaterials, based on the intuition that the Janus coating of enzymes can generate driving force from asymmetric catalytic reactions. Here, in the fabrication of catalase-powered silica micro/nanomotors (C-MNMs), an archetypical model of enzyme-powered micro/nanomotors, we find the silica size rather than asymmetric coating of catalase determines the motion ability of C-MNMs. The effects of size and asymmetry have been investigated by a series of C-MNMs at various sizes (0.5, 2, 5 and 10 μm) and asymmetric levels (full-, half- and most-coated with catalase). The motion performance indicates that 500 nm and 2 μm C-MNMs show obvious increases (varying from 134% to 618%) of diffusion coefficient, but C-MNMs bigger than 5 μm have no self-propulsion behaviour at all, regardless of asymmetric levels. In addition, although asymmetry facilitates enhanced diffusion of C-MNMs, only 2 μm C-MNMs are sensitive to asymmetric level. This work elucidates the primary and secondary roles of size and asymmetry in the preparation of C-MNMs, paving the way to fabricate enzyme-powered micro/nanomotors with high motion performance in future.

Introduction

Synthetic micro/nanomotors (MNMs) that can convert energy from the environment into momentum to perform autonomous motion and proactive dynamic tasks are attracting widespread interest.[1] For example, with the rapid development of micro- and nanofabrication technologies, MNMs have been applied and made breakthroughs in the fields of environmental monitoring and remediation,[2] biosensing,[3] drug delivery,[4] micro-therapy,[5] and cluster and communication studying.[6] To date, multifarious MNMs of different shapes (such as Janus microspheres, nanowires, microtubes, microshells, microhelix, nanotree and other irregular shapes), materials (such as silica, metal, polymer, liquid metal, metal–organic framework and enzyme) and driving forces (such as chemical/biochemical reactions, acoustic waves, light, magnetic and electric fields) have been prepared.[7–11] Among them, chemically driven MNMs have been extensively studied as they can move autonomously and independently by harvesting chemical energy from the fuel environment, without the requirement of external equipment for real-time stimuli.[12,13] In addition to active metals such as magnesium- and zinc-based MNMs,[14,15] chemically driven MNMs are mainly catalytic motors.

One typical design of catalytic MNMs is Janus microsphere with half coating of catalyst, for example, catalytic metal and enzymes, to asymmetrically decompose fuel molecules and generate propulsion.[16] The reported catalyst/fuel pairs include Pt/H_2O_2, Ir/N_2H_4, catalase/H_2O_2, urease/urea and glucose oxidase/glucose.[16–18] Among them, Pt-coated MNMs (Pt-MNMs) are commonly used as models to study the preparation and movement mechanisms of catalytic MNMs.[19–21] However, as the Pt-MNMs usually need high concentration of H_2O_2 (>1%) which is bio-unfriendly, enzyme-powered MNMs have received mounting interest,[22,23] especially in the fields of biology and biomedicine.

Catalase has good stability and high catalytic activity, and can convert H_2O_2 rapidly to O_2 with a high turnover rate of ~10^5 molecules per second,[24] which is comparable to the most active Pt, thus, catalase-powered MNMs (C-MNMs) have been widely prepared according to the models of Pt-MNMs.[25–27] However, for the sphere-shaped MNMs, Pt-MNMs have been fabricated normally with a half-coated Janus design, but there are divergent opinions on the preparation of C-MNMs. For example, Sánchez's group prepared C-MNMs with 400 nm hollow mesoporous silica nanoparticles based on the half-coated Janus design,[28] but Sen's group reported the fabrication of C-MNMs on 2 μm polystyrene microspheres with a non-Janus design in which catalase was fully coated without any asymmetric modification.[29] In addition, Wang and Ma's group proposed that the Janus modification of catalase on 5 μm silica microspheres was unable to prepare C-MNMs with motion performance.[21] Although there is a general cognition in MNMs that its motion performance is influenced by size and asymmetry,[30,31] it is still important to make clear how these two factors affect the fabrication design as well as the performance of C-MNMs.

In this article, we fabricated a series of silica-based C-MNMs with different sizes and asymmetric levels to explore the effect of size and asymmetry on C-MNMs. The results showed C-MNMs bigger than 5 μm would completely lose their motion perform-

[a] J. Sun, Prof. J. Wu, Prof. H. Ju
State Key Laboratory of Analytical Chemistry for Life Science
School of Chemistry and Chemical Engineering
Nanjing University, 163 xianlin Road, Nanjing 210023 (P. R. China)
E-mail: wujie@nju.edu.cn

Supporting information for this article is available on the WWW under https://doi.org/10.1002/asia.202300900

ance, regardless of asymmetric levels. In addition, C-MNMs at both 500 nm and 2 μm could show enhanced diffusion with asymmetric fabrication, however, only the latter's motion performance was sensitive to the asymmetric level. This work clearly indicated that its size rather than asymmetry determined the motion ability of C-MNMs, which provided a clear guidance for the preparation of enzyme-powered MNMs.

Results and Discussion

Effect of asymmetry on the motion performance of 500 nm C-MNMs

The biological and biomedical applications are driving the fabrication of MNMs with smaller sizes (<1 μm) and lower fuel concentrations (approaching physiological concentration). Generally, asymmetric design is considered as the primary factor in the preparation of MNMs, however, this viewpoint has been challenged in the fabrication of enzyme-powered MNMs, especially those with sphere shapes and sizes smaller than 5 μm.[31] We speculated that it might be because the enzymatic reactions of low concentration fuels (near physiological concentrations) could only produce very small driving forces, making them more susceptible to the influence of size dependent viscosity and gravity, rather than the asymmetric coating of enzymes. To verify this opinion, we fabricated three types of C-MNMs with different asymmetric levels, namely full-coated C-MNMs, half-coated C-MNMs and most-coated C-MNMs, to investigate the effect of asymmetry on the motion performance of 500 nm silica-based C-MNMs with low concentration fuels (0–30 mM H_2O_2). Here, the full-coated, half-coated and most-coated C-MNMs were fabricated by coupling catalase on untreated, Au-half-coated and PEG-dot-coated amino-functionalized silica microspheres (SiO_2-NH_2 MPs) via glutaraldehyde (GA) linker, respectively (Figure 1A). The coating levels of catalase on the three types of C-MNMs were observed by fluorescence imaging (Figure 1B, C and D). As expected, the characterization results were consistent with the design of C-MNMs, for example, the full coating of catalase on the whole spherical surface of silica was observed for full-coated C-MNMs (Figure 1B). In addition, the half-coated C-MNMs showed an obvious half-moon-shaped fluorescence distribution, indicating the half coating of catalase on its surface, this result was also confirmed by the SEM characterization of Au-half-coated SiO_2-NH_2 MPs (Figure 1C). For the most-coated C-MNMs, as PEG only reacted with the amino groups on the dot section of MPs (1% of the sphere area according to the spherical crown formula), so theoretically, 99% spherical surface of silica would be coated with catalase, resulting in a full cover of fluorescence on its surface similar to that of full-coated C-MNMs (Figure 1D).

Typical motion trajectories of the three types of C-MNMs were recorded by optical microscopy (Figure 1E, G, I, Videos S1, S2, S3), and the mean squared displacement (MSD) curves

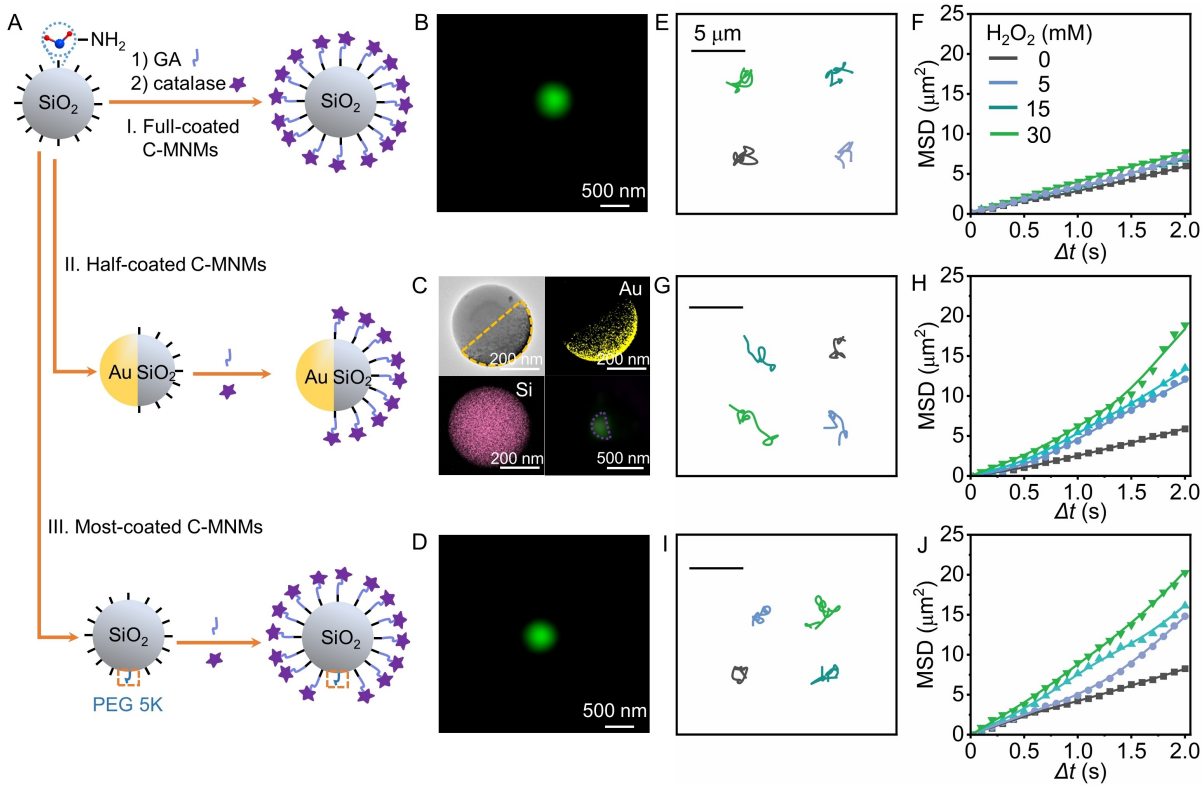

Figure 1. (A) Schematic illustration of the fabrication of full-coated, half-coated and most-coated C-MNMs. Fluorescent and SEM images of 500 nm (B) full-coated, (C) half-coated and (D) most-coated C-MNMs. Motion trajectories (duration: 5 s) and MSD curves of 500 nm (E, F) full-coated, (G, H) half-coated and (I, J) most-coated C-MNMs under different H_2O_2 concentrations.

versus time interval (Δt) were plotted according to the trajectories (Figure 1F, H, J). MSD analysis is a reliable quantification tool for evaluating the dynamics of a specific colloidal particle, thus distinguishing it from a common Brownian particle.[32] For full- coated C-MNMs, no obvious difference of MSD was observed by increasing fuel (H_2O_2) concentration from 0 to 30 mM (Figure 1F). However, a significant increase (nearly 3-fold) of MSD was observed on both half-coated and most-coated C-MNMs (Figure 1H and J). These results indicated that the asymmetric modification of enzymes to generate unbalanced forces was essential for the fabrication of active C-MNMs at 500 nm, but there was no strict requirement for the degree of asymmetry, even 1% asymmetric design could activate full motion ability of 500 nm C-MNMs. This could explain why some reported full-coated non-Janus enzyme MNMs had motion performance,[28,29] it might be due to the small degree of asymmetry caused by the imperfect template materials and modification processes.

Motion performance of half-coated C-MNMs at different sizes

The above results showed that the half-coated and most-coated C-MNMs at 500 nm presented a similar MSD increase from 0 to 30 mM H_2O_2. In order to investigate whether this phenomenon existed on other sizes of C-MNMs, we further investigated the motion performance of half-coated and most-coated C-MNMs at 2, 5 and 10 μm, respectively. The fabrication of half-coated C-MNMs at different sizes were characterized by SEM and fluorescence. The clear Au-half-coated Janus morphologies (Figure 2A, C and E) and half-moon-shaped fluorescence distributions (Figure 2B, D and F) suggested the successful fabrication of half-coated C-MNMs at 2, 5 and 10 μm. Afterward, we tracked the motion of these half-coated C-MNMs under different fuel concentrations and found that only 2 μm C-MNMs showed long trajectories and obvious enhanced MSD in 30 mM H_2O_2 (Figure 2G, H and Video S4). No motion ability was observed on half-coated C-MNMs at both 5 and 10 μm in the fuel solution (Figure 2I, J, K, L, Videos S5 and S6). This result indicated that the preparation of C-MNMs had significant size limitation (< 5 μm). This result was also consistent with the results reported in the literature,[21] that was, it was unable to prepare active C-MNMs at 5 μm with a half-coated Janus design.

Motion performance of most-coated C-MNMs at microscales

The most-coated C-MNMs at 2, 5 and 10 μm were fabricated by using the corresponding size PEG-dot-coated SiO_2-NH_2 MPs. According to the spherical crown formula, the coverage ratio of PEG would decrease with the increase of silica size, conversely, the coverage ratio of catalase would gradually approach 100% from 500 nm to 10 μm. So, similar to 500 nm C-MNMs (Figure 1D), the most-coated C-MNMs at 2, 5 and 10 μm all showed full cover of fluorescence on their surfaces (Figure 3A, B and C). Likewise, their motion performances were visualized and quantified by trajectories and MSD curves. Similar to that of half-coated C-MNMs, only 2 μm most-coated C-MNMs displayed obvious self-propulsion (Figure 3D, Video S7) and increased

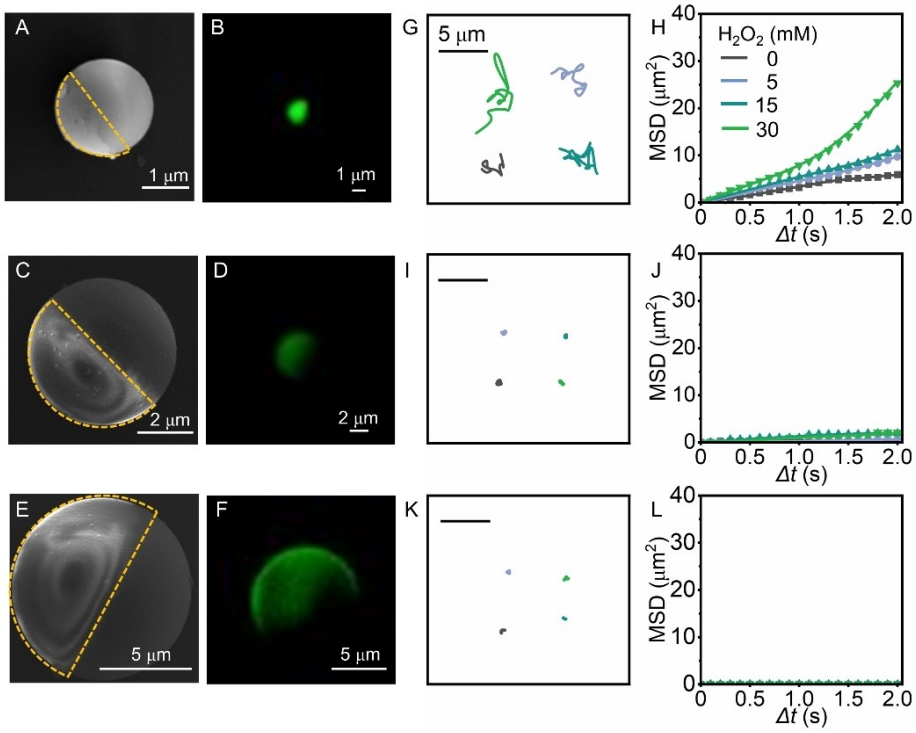

Figure 2. SEM (A, C, D) and fluorescent (B, D, F) images, motion trajectories (G, I, K) (duration: 5 s) and MSD curves (H, J, L) of half-coated C-MNMs at sizes of (A, B, G, H) 2 μm, (C, D, I, J) 5 μm and (E, F, K, L) 10 μm.

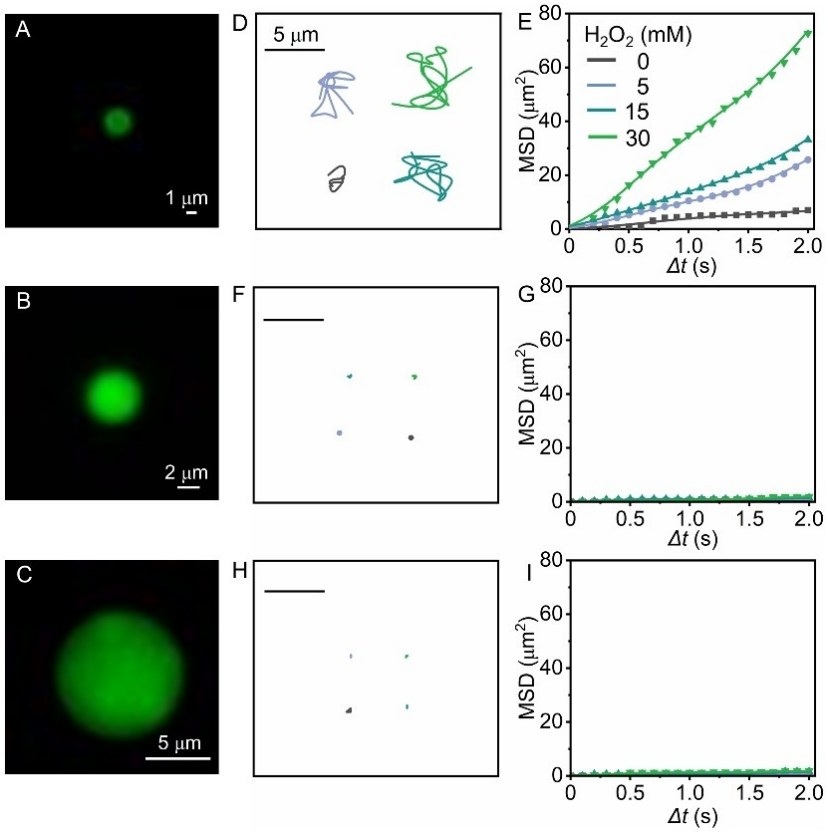

Figure 3. Fluorescent images (A, B, C), motion trajectories (duration: 5 s) (D, F, H) and MSD curves (E, G, I) of most-coated C-MNMs with diameters of (A, D, E) 2 μm, (B, F, G) 5 μm and (C, H, I) 10 μm.

MSD tendency (Figure 3E) in 5–30 mM H_2O_2 compared with that in the absence of H_2O_2. Neither 5 μm (Figure 3F, G and Video S8) nor 10 μm (Figure 3H, I and Video S9) most-coated C-MNMs present motion ability in the fuel solutions. This result also indicated that the motion ability of C-MNM had significant size limitation (< 5 μm).

The decisive factor in the motion ability of C-MNMs

In order to have a clear understanding of the impact of size and asymmetry on the motion ability of C-MNM, we compared the effective diffusion coefficient (D_e, calculated from $D_e = \mathrm{MSD}/4\Delta t$) of half-coated and most-coated C-MNMs in 0 and 30 mM H_2O_2 with sizes from 0.5 to 10 μm (Figure 4). For C-MNMs at sizes of 0.5 and 2 μm, whether they were designed to be half-coated or most-coated with catalase, a significant enhancement of D_e (varying from 134% to 618%) was observed in 30 mM H_2O_2 compared with that in the absence of H_2O_2. On the contrary, for both types of C-MNMs at sizes of 5 and 10 μm, no enhanced D_e was observed in the presence of 30 mM H_2O_2. Additionally, it should be noted that the Brownian motion in both 5 and 10 μm C-MNMs was not significant, and their D_e was much lower than those of C-MNMs at sizes of 0.5 and 2 μm. It should be due to the huge drag force from the fluid. The drag force of the fluid on a spherical colloid can be quantified based on the Stokes equation of $F_{drag} = 6\pi\eta rv$, where η is the viscosity of water, r is the radius of spherical motor and v is the velocity of motor. As the proportional relationship between the drag force and motor size, the drag forces of 5 and 10 μm C-MNMs were greater than

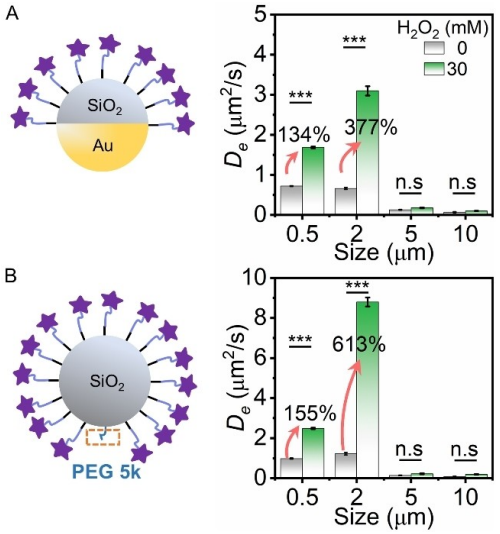

Figure 4. Comparison of D_e of (A) half-coated and (B) most-coated C–MNMs at different sizes. A t-test was used to compare the differences of experimental groups. The asterisks (*) denote statistical differences: ***$p < 0.001$, $p > 0.05$ represents not significant (n.s).

that of 0.5 and 2 μm motors. Therefore, for 5 and 10 μm C-MNMs, the small driving forces generated by enzymatic reaction were not adequate to balance the big drag forces, resulting in a complete lack of mobility regardless of asymmetric levels. This result suggested that the motor size determined the motion ability of C-MNM.

Additionally, for 0.5 and 2 μm C-MNMs, although enhanced diffusion motion was observed in both half-coated and most-coated C-MNMs, the D_e of the latter (155% and 613%, Figure 4B) showed a greater increase than the former (134% an 377%, Figure 4A) in 30 mM H_2O_2, especially for 2 μm C-MNMs (613% *vs* 377%). Here, the greater increase of D_e in the most-coated C-MNMs should be mainly attributed to a bigger driving force from the larger amounts of enzymes and a smaller drag force from the lighter material compared to the Au-half-coated C-MNMs. In addition, the phenomenon that 2 μm C-MNMs were more sensitive to asymmetry than 0.5 μm C-MNMs could be attributed to the threshold behavior of motion performance.[33]

As we mentioned above, for 2 μm most-coated C-MNMs, the catalase coverage was >99%, which could be achieved through the imperfect template materials and modification processes. So, in other words, as long as the size of C-MNMs was ensured to be 2 μm, it could have motion ability without the need of deliberate asymmetric design. This result also suggested that the decisive factor in the preparation of C-MNMs was the size of silica rather than the asymmetric modification of enzymes.

Active colloidal motors without precise asymmetry

To verify the primary role of size in C-MNMs, we further investigated and compared the motion performances of three kinds of 2 μm C-MNMs, including a kind of full-coated C-MNMs (Figure 5A), and two kinds of most-coated C-MNMs prepared using 5 K and 10 K PEG (Figure 5B and C), respectively. For all the three kinds of 2 μm C-MNMs, the plotted MSD curves displayed increasing tendencies versus time interval from 0 to 30 mM H_2O_2 (Figure 3E, 5D and E). D_e analysis showed the full-coated C-MNMs could present a 198% enhancement in 30 mM H_2O_2 (Figure 5D), confirming the 2 μm C-MNMs could have motion ability without any asymmetric design.

Additionally, greater enhancement of D_e was observed in both kinds of most-coated C-MNMs (613% and 618%) (Figure 4B and 5E). AFM characterization showed that 5 K and 10 K PEG could form molecule layers with thickness of ~6 nm and ~8 nm, respectively, on the slides (Figure 5C). It should be noted that although AFM can intuitively display the morphology of the interface, it cannot display the true morphology of the interface due to the limited scanning area. According to the spherical crown area formula and the silica size of 2 μm, theoretical catalase coverages of C-MNMs prepared using 5 K and 10 K PEG were 99.7% and 99.6%, respectively. Compared to the full-coated C-MNMs, the most-coated C-MNMs had only 0.3–0.4% increase in asymmetry, but their motion ability enhanced three folds (613% & 618% *vs* 198%), indicating that a tiny asymmetry could facilitate the motion ability of C-MNMs. Moreover,

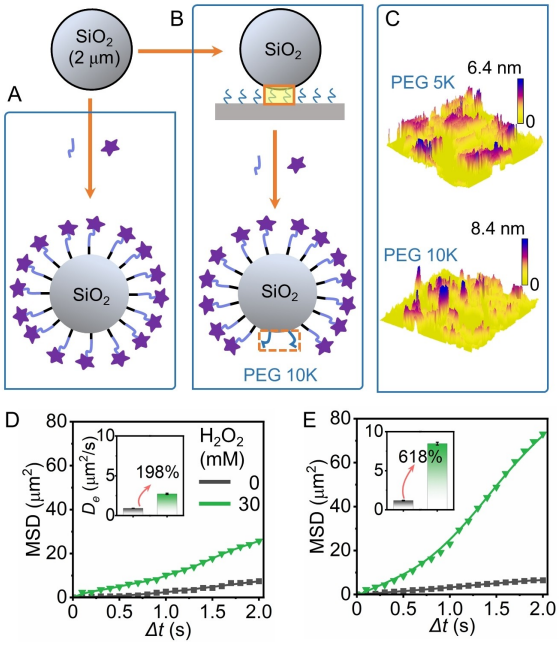

Figure 5. Illustrated fabrication of 2 μm (A) full-coated C-MNMs and (B) most-coated C-MNMs. (C) AFM characterization of the thickness of 5 K and 10 K PEG layers. MSD curves inserted with D_e of (D) full-coated C-MNMs and (E) most-coated C-MNMs using 10 K PEG.

comparing the D_e of the two kinds of most-coated C-MNMs, no significant difference was observed (613% *vs* 618%), suggesting precision asymmetric design could not further enhance the motor motion. The overall results clarified the primary and secondary roles of size and asymmetry in the preparation of silica-based C-MNMs.

Conclusions

In summary, this work explored the role of silica size and asymmetric level of catalase coating in the fabrication of active C-MNMs. The motion ability of a series of C-MNMs at different sizes (0.5, 2, 5 and 10 μm) and asymmetric designs (full-coated non-Janus design, half-coated typical-Janus design and most-coated dot-Janus design) were investigated and compared by analysing their trajectories, MSD curves and diffusion coefficients. 2 μm C-MNMs always exhibited the best motion ability and greatest enhancement of D_e, while 5 and 10 μm C-MNMs would lose completely their motion ability due to the big drag force from viscosity and gravity, regardless of the asymmetric designs. In addition, except for the Janus C-MNMs, the full-coated non-Janus C-MNMs at the size of 2 μm also presented motion ability with an increase of 198% of D_e in 30 mM H_2O_2. Compared to the non-Janus C-MNMs, both half-coated and most-coated C-MNMs exhibited better motion ability, especially, D_e of most-coated C-MNMs increased by 613% which was much better than 377% for half-coated C-MNMs. These results indicated that the silica size was the primary factor that determined the motion ability of C-MNMs, and at the optimal motor size (2 μm), asymmetric design, whether half-coated

typical-Janus design or most-coated dot-Janus design, could promote an increase in the mobility of C-MNM. These findings could guide the fabrication of enzyme-powered MNMs with high motion performance. However, for the fabrication of efficient enzyme-powered nanomotors, future research may focus more on developing C-MNMs with designed shapes (such as nanoflask, nanojet and nanotree) and hybrid propulsion (such as the combination of self-electrophoresis and self-diffusiophoresis).

Experimental section

Fabrication of full-coated C-MNMs

1 mg SiO_2-NH_2 MPs (from Shanghai Aladdin Bio-Chem Technology Co., Ltd.) at size of 500 nm were dispersed in 200 μL phosphate buffered saline (PBS, 0.1 M, pH 7.2) containing 50 mM glutaraldehyde (GA) for 2 h. Then, the MPs were washed by centrifugation and dispersed in 200 μL PBS containing catalase (5 mg/mL) for 2 h reaction under slight oscillation at room temperature. GA served as a linker to conjugate catalase on SiO_2-NH_2 MPs. After complete wash with centrifugation, full-coated C-MNMs were obtained and re-dispersed in pure water. They were stored at 4 °C for further use.

Fabrication of half-coated C-MNMs

The half-coated C-MNMs were prepared via template-directed deposition. Before deposition, SiO_2-NH_2 MPs (0.5, 2, 5 and 10 μm) dispersed in ethanol were dropped onto glass slides pretreated with Piranhas acid. Then, a monolayer as a template formed after ethanol was volatilized at room temperature. By using an e-beam evaporation system (Kurt J. Lesker PVD75 Prolin), 10 nm Au was half coated on SiO_2-NH_2 MPs. After that, the Au-half-coated MPs were collected by a slight ultrasonication and suspended in PBS for half coating of catalase by GA through the similar fabrication procedure of full-coated C–MNMs described above.

Fabrication of most-coated C-MNMs

Firstly, the polyethylene glycol (HS-PEG-NH_2, 5 kD and 10 kD, Shanghai ToYong Bio Tech. Inc. China) coated slides were prepared based on Schiff's base reaction between amino and aldehyde groups. Briefly, 200 μL 1 mg/mL HS-PEG-NH_2 (in PBS) was dropped on aldehyde-functionalized glass slides at room temperature for 2 h reaction. After washing with pure water and drying, the PEG coated slides were obtained. Then, 200 μL 3 mM 3-maleimidobenzoic acid N-hydroxysuccinimide ester (MBS) was dropped on the sides for 1 h to form PEG-MBS. After washing and drying, the slides were covered with 200 μL SiO_2-NH_2 MPs (0.5, 2, 5 and 10 μm) for 1 h to form PEG-SiO_2 MPs on the surface of slides. After rinsing away the unreacted MPs, the PEG-SiO_2 MPs were detached from the slides with tweezers. Due to the fact that the thickness of the PEG layer was much smaller than the size of SiO_2-NH_2 MPs, PEG would be only linked on the dot section of MPs where it contacted the slides. These PEG-dot-coated MPs were collected and suspended in PBS for most coating of catalase by GA through the similar fabrication procedure of full-coated C-MNMs described above.

Functionalization of catalase with FITC

1 mL PBS (0.1 M, pH 9.2) containing 20 mg catalase and 0.5 mg FITC (Shanghai Macklin Biochemical Co., Ltd. China) were prepared and incubated for 4 h with slight shaking in the dark. The FITC labelled catalase was obtained after removing the excess FITC molecules by putting the solution into a dialysis membrane (3.5 kDa pore membrane) in PBS (0.1 M, pH 7.2) for 24 h.

Calculation of the coating rate of catalase on most-coated C-MNMs

The coating rate of catalase on most-coated C-MNMs is calculated by $[(S_{sphere}\text{-}S_{crown})/S_{sphere}]\%$, where $S_{sphere}=4\pi r^2$ and $S_{crown}=2\pi rh$ (spherical crown formula). Here, r is the radius of SiO_2 MP and h is the thickness of PEG (6.4 nm for 5 K PEG and 8.4 nm for 10 K PEG).

Characterizations

Scanning electron microscopy (SEM) images were obtained using a field emission SEM (JEOL JSM-7800F, Japan). Fluorescent photographs were obtained by an inverted microscopy (Leica DMi8, Germany) with a CCD camera (Andor-iXon Ultra). Surface morphology of PEG coated slides was imaged by Atomic Force Microscopy (AFM) (Bruker Icon). An inverted optical microscope (Leica, DMI 3000B) equipped with a Photometrics Evolve 512/SC camera (Roper Scientific, Duluth, GA) at a frame rate of 10 frames/s was used to obtain trajectories of the motors. Motor stock solution was mixed with the fuel solutions of different concentrations of H_2O_2 and 0.8% NaCh at a volume ratio of 1:10. In order to minimize fluid drift effect, the mixture solution was placed under a microcap and the total volume was controlled at 6 μL. More than 3 typical particles were tracked to plot MSD-Δt curves. The MSD was calculated by MSD $(\Delta t)=[(x_i(t+\Delta t)-x_i(t))^2]$ ($i=2$, for two-dimensional analysis).

Acknowledgements

We gratefully acknowledge the Independent Research Foundation from State Key Laboratory of Analytical Chemistry for Life Science (5431ZZXM2006).

Conflict of Interests

The authors declare no conflict of interest.

Data Availability Statement

The data that support the findings of this study are available in the supplementary material of this article.

Keywords: asymmetry · catalase · micro/nanomotors · silica · size

[1] T. Y. Liu, L. Xie, C.-A. H. Price, J. Liu, Q. He, B. Kong, *Chem. Soc. Rev.* **2022**, *51*, 10083.
[2] H. Q. Shi, X. Chen, K. Liu, X. Y. Ding, W. J. Liu, M. L. Xu, *J. Colloid Interface Sci.* **2020**, *572*, 39–47.
[3] X. Q. Zhang, C. T. Chen, J. Wu, H. X. Ju, *ACS Appl. Mater. Interfaces* **2019**, *11*, 13581–13588.
[4] M. M. Wan, T. Li, H. Chen, C. Mao, J. Shen, *Angew. Chem. Int. Ed.* **2021**, *60*, 13158–13176.
[5] Y. Feng, C. Gao, D. Z. Xie, L. Liu, B. Chen, S. Y. Liu, H. H. Yang, Z. Gao, D. A. Wilson, Y. F. Tu, F. Peng, *Adv. Mater.* **2023**, *35*, 2301736.

[6] Z. Yu, L. L. Li, F. Z. Mou, S. M. Yu, D. Zhang, M. Y. Yang, Q. Zhao, H. R. Ma, W. Luo, T. L. Li, J. G. Guan, *InfoMat.* **2023**, e12464.
[7] H. Wang, M. Pumera, *Chem. Rev.* **2015**, *115*, 8704–8735.
[8] F. Soto, E. Karshalev, F. Y. Zhang, B. Esteban-Fernández de Ávila, A. Nourhani, J. Wang, *Chem. Rev.* **2022**, *122*, 5365–5403.
[9] H. B. Ge, X. Chen, W. J. Liu, X. L. Lu, Z. W. Gu, *Chem. Asian J.* **2019**, *14*, 2348–2356.
[10] M. You, C. R. Chen, L. L. Xu, F. Z. Mou, J. G. Guan, *Acc. Chem. Res.* **2018**, *51*, 3006–3014.
[11] T. Y. Liu, L. Xie, J. Zeng, M. Yan, B. L. Qiu, X. Y. Wang, S. Zhou, X. Zhou, H. Zeng, Q. R. Liang, Y. J. He, K. Liang, J. Liu, E. Velliou, L. Jiang, B. Kong, *ACS Appl. Mater. Interfaces* **2022**, *14*, 15517–15528.
[12] S. Sánchez, L. Soler, J. Katuuri, *Angew. Chem. Int. Ed.* **2015**, *54*, 1414–1444.
[13] Y. H. Zheng, H. Zhao, Y. P. Cai, B. J. Sanchez, R. F. Dong, *Nano-Micro Lett.* **2023**, *15*, 20.
[14] C. Xu, S. H. Wang, H. Wang, K. Liu, S. Y. Zhang, B. Chen, H. Liu, F. Tong, F. Peng, Y. F. Tu, Y. J. Li, *Nano Lett.* **2021**, *21*, 1982–1991.
[15] Z. H. Lin, C. Y. Gao, D. L. Wang, Q. He, *Angew. Chem. Int. Ed.* **2021**, *60*, 8750–8754.
[16] J. R. Howse, R. A. L. Jones, A. J. Ryan, T. Gough, R. Vafabakhsh, R. Golestanian, *Phys. Rev. Lett.* **2007**, *99*, 048102.
[17] W. Gao, A. Pei, R. F. Dong, J. Wang, *J. Am. Chem. Soc.* **2014**, *136*, 2279–2279.
[18] X. Ma, X. Wang, K. Hahn, S. Sánchez, *ACS Nano* **2016**, *10*, 3597–3605.
[19] X. L. Lyu, J. Y. Chen, J. Y. Liu, Y. X. Peng, S. F. Duan, X. Ma, W. Wang, *Angew. Chem. Int. Ed.* **2022**, *61*, e202201018.
[20] Y. X. Peng, P. Z. Xu, S. F. Duan, J. Y. Liu, J. L. Moran, W. Wang, *Angew. Chem. Int. Ed.* **2022**, *61*, e202116041.
[21] X. L. Lyu, X. X. Liu, C. Zhou, S. F. Duan, P. Z. Xu, J. Dai, X. C. Chen, Y. X. Peng, D. H. Cui, J. Y. Tang, X. Ma, W. Wang, *J. Am. Chem. Soc.* **2021**, *143*, 12154–12164.
[22] X. Ma, A. C. Hortelão, T. Patiño, S. Sánchez, *ACS Nano* **2016**, *10*, 9111–9122.
[23] H. Yuan, X. X. Liu, L. Y. Wang, X. Ma, *Bioact. Mater.* **2021**, *6*, 1727–1749.
[24] S. Sengupta, D. Patra, I. Ortiz-Rivera, A. Agrawal, S. Shklyaev, K. K. Dey, U. Cordova-Figueroa, T. E. Mallouk, A. Sen, *Nat. Chem.* **2014**, *6*, 415–422.
[25] C. T. Chen, Z. Q. He, J. Wu, X. Q. Zhang, Q. F. Xia, H. X. Ju, *Chem. Asian J.* **2019**, *14*, 2491–2496.
[26] D. A. Wilson, R. J. M. Nolte, J. C. M. V. Heat, *Nat. Chem.* **2012**, *4*, 268–274.
[27] L. K. E. A. Abdelmohsen, M. Nijemeisland, G. M. Pawar, G–J. A. Janssen, R. J. M. Nolte, J. C. M. V. Hest, D. A. Wilson, *ACS Nano* **2016**, *10*, 2652–2660.
[28] X. Ma, A. Jannasch, U–R. Albrecht, K. Hahn, A. Miguel-López, E. Schaffer, S. Sánchez, *Nano Lett.* **2015**, *10*, 7043–7050.
[29] K. K. Dey, X. Zhao, B. M. Tansi, W. J. Méndez-Ortiz, U. M. Córdova-Figueroa, R. Golestanian, A. Sen, *Nano Lett.* **2015**, *15*, 8311–8315.
[30] Y. Xing, Q. Pan, X. Du, T. L. Xu, Y. He, X. J. Zhang, *ACS Appl. Mater. Interfaces* **2019**, *11*, 10426–10433.
[31] T. Patiño, X. Arque, R. Mestre, L. Palacios, S. Sánchez, *Acc. Chem. Res.* **2018**, *51*, 2662–2671.
[32] X. Chen, C. Zhou, W. Wang, *Chem. Asian J.* **2019**, *14*, 2388–2405.
[33] T. Patiño, N. Feiner-Gracia, X. Arqué, A. Miguel-Lopez, A. Jannasch, T. Stumpp, E. Schaffer, L. Albertazzi, S. Sánchez, *J. Am. Chem. Soc.* **2018**, *140*, 7896–7903.

Manuscript received: October 12, 2023
Revised manuscript received: November 6, 2023
Accepted manuscript online: November 22, 2023
Version of record online: ■■, ■■

RESEARCH ARTICLE

The role of silica size and asymmetric level of catalase coating in the fabrication of active ocatalase-powered silica micro/nanomotors (C-MNMs) has been investigated. The results indicated that the silica size is the primary factor that determines the motion ability of C-MNMs.

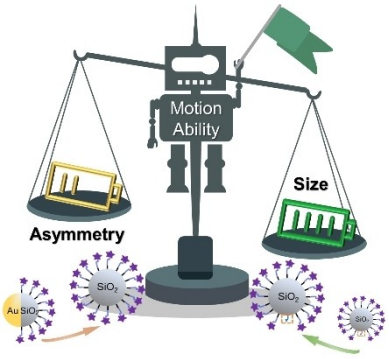

J. Sun, Prof. J. Wu, Prof. H. Ju*

1 – 8

Effects of Size and Asymmetry on Catalase-Powered Silica Micro/nanomotors